Evaluating Ionizer Efficiency Using a Discharge Current Sensor

Ellen Merkel (1), Heinrich Wolf (1), Leon Heiland (1), Joshua Yoo (2), Elly Koo (2), Amelie Hagelauer (1, 3)

(1) Fraunhofer EMFT, Hansastr. 27 d, 80686 Munich, Germany
tel.: +498954759-533, e-mail: ellen.merkel@emft.fraunhofer.de

(2) Core Insight, Inc., Seongnam Central Biz Tower Phase 3, 208 Glamachi-ro, Jungwon-gu, Seongnam-si, Gyeonggi-do 13216, Korea

(3) Chair of Micro- and Nanosystems Technology, Technical University of Munich, Arcisstr. 21, 80333 Munich, Germany

Abstract - This paper presents a method to characterize bar ionizers using the discharge current sensor and aluminum DUTs. The DUT is held and moved in Z-direction by a pick & place head and exposed to DC or AC bar ionizer. The frequency of the AC ionizers, DUT size, distance between the DUT and the ionizer and the DC offset are varied. Without pre-charging the DUT, low-frequency AC ionizer produced the highest peak currents. Larger DUTs and greater separation increases the peak currents. With 100 V pre-charging, both ionizers reduce the charge effectively, with lower peaks for DC. The approach complements charged plate monitor tests for short-timescale and low offset voltage performance.

I. Introduction

Ionizers are an essential element of every ESD process assessment, as they offer the only possibility to eliminate accumulated charge on insulators [1, 2]. However, if not well maintained and balanced, they can even charge up their environment including the Electrostatic Discharge Sensitive Devices (ESDS).

For this reason, ANSI/ESD STM3.1 and ANSI/ESD SP3.3 were developed which discuss how to install the ionizers and measure their efficiency and offset [3], or how to verify them periodically [4, 5]. For this purpose, a so-called Charged Plate Monitor (CPM) is used, which contains an electrode with the size of 15 cm by 15 cm, a ground electrode, voltage source and a voltmeter or electrometer. Using the CPM, the Discharge Time Test as well as the Offset Voltage Test can be performed [3]. The first monitors the time needed to discharge the CPM to 10 % of an initial voltage, the latter monitors the CPM voltage in the presence of ionized air flow for the time interval of 1 to 5 minutes (for bar ionizers) [3]. However, the sensitivity of the measurements is strongly dependent on the performance of the volt-/electrometer. Moreover, the electrode of the CPM is rather large, which arises the question, whether the measurements described in [3] are suitable for modern processes including heterogenous integration.

while [6] discusses how to achieve a sub-1 V balanced environment, the presented measurements are limited to longer time scales. Furthermore, previous work [7]-[9] has shown that standard CPM technology is limited to evaluating AC ionizers, as its response time is insufficient to accurately capture the behavior of high-frequency AC ionizers. The authors suggested to connect the CDM to a high-speed oscilloscope to enable more accurate measurements. However, none of these studies investigated whether and how ionizers can charge a device on a very short time scales, as mentioned in [10]. In this work, we aim to bridge this gap. This is especially important given the growing interest in advanced packaging technologies and die to die and die to wafer stacking.

II. Methodology

This section discusses the measurement setup (II.A.) followed by the description of the devices under test (DUT) in II.B. Finally, the section is concluded with the specification of the performed measurements (II.C.).

A. Measurement setup

Fig. 1 presents the measurement setup. It consists of a bar ionizer, which is placed in a distance of 15 cm from the DUT (if not stated differently), with the

nozzles facing the DUT. The pick & place head, which is positioned above the discharge current sensor (DCS), holds the DUT with an insulative nozzle and places the DUT on the pogo-pin of the DCS, similarly to the measurements in [11, 12]. One microstrip line of the DCS is connected to a 33 GHz oscilloscope, the other line to a DC voltage source. With the exception of section III.F, where the DUT is additionally pre-charged to 100 V, only the discharge part of the DCS connected to an oscilloscope is used.

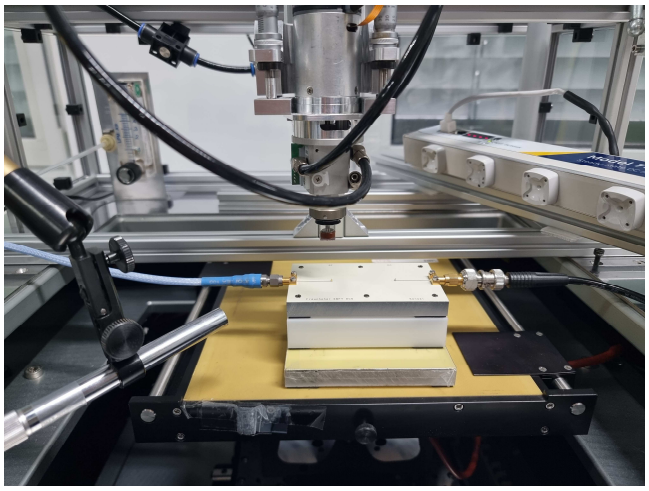

Figure 1: Measurement setup

B. Devices Under Test

The DUTs chosen for this study are solid aluminum plates. Three sizes were tested: 10 mm x 10 mm, 15 mm x 15 mm and finally 40 mm x 40 mm, all with the thickness of 1.5 mm (Fig. 2, from left to right). The smaller DUTs emulate chips and chiplets for the integration into Multi-Chip Modules (MCM), while the largest size was chosen to mimic a large GPU/CPU chip. Solid metal plates are chosen so that the ions have access to the DUT from both the top and the bottom side.

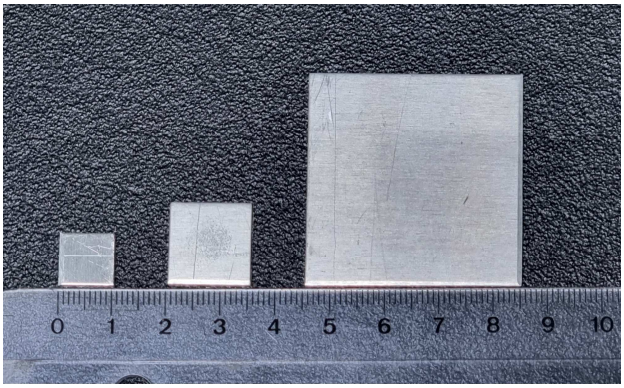

Figure 2: DUTs used for this study, from the left to right: 10 mm, 15 mm and 40 mm edge length

C. Ionizers

Four different bar ionizers are used in this study, as summarized in Table 1. The AC ionizers B and C utilize alternating polarity on the same nozzle, with a tunable frequency at which the polarity alternates. The AC ionizer A operates at fixed frequency. The DC ionizer (Table 1, D) incorporates 4 emitters per nozzle, two which emit positive ions and the remaining two negative ions. The AC ionizers B and C use alternating polarity of ions on the same nozzle. The frequency at which the polarity changes is tunable. The AC ionizer A operates at fixed frequency.

Table 1: Overview of used ionizers

NAME OF THE IONIZER	IONIZER TYPE	FREQUENCY	OFFSET VOLTAGE
A	AC	Fixed	-
B	AC	Variable	-
C	AC	Variable	-
D	DC	-	Variable

D. Data analysis

For each measurement, 100 discharges are performed. All triggered data are than summarized as box-and-whiskers plot. The most important term within the plot is a quartile: one fourth of all acquired and ordered measured data set. Fig. 3 illustrates a schematic depiction of a box-whiskers plot as being used in the following chapters. It consists of a box, which depicts the lower quartile (Fig. 3, Q1) and the upper quartile (Fig. 3, Q3). The median (Fig. 3, Q2) is always highlighted in color, as it depicts the middle value where 50% of datapoints falls below it and 50% above it. The box is connected to the whiskers, vertical lines ending with the lower extreme (Fig. 3, Q1-1.5(Q3-Q1)) and upper extreme (Fig. 3, Q3+1.5(Q3-Q1)). The outliers, which do not lie within these values are marked with a circle.

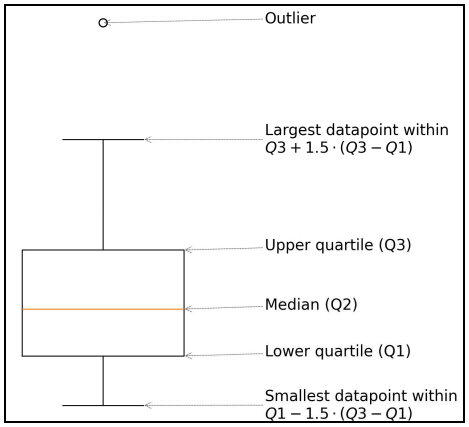

Figure 3: Schematic illustration of a box-and-whisker plot, showing the definition of its key components

E. Influence of the oscilloscope setup

The oscilloscope setup significantly influences the measurement results. When the Volts per division (V/div) setting is low, most discharge pulses exceed the trigger threshold and are captured. However, larger discharge pulses are clipped, which artificially lowers the median. On the other hand, with a high V/div setting, low-amplitude discharge pulses fall below the trigger threshold and are not measured, leading to an artificially elevated median. The difference of the captured peak currents for these two settings is presented in Fig. 4, on the example of a 10 mm. In the plot, the V/div values have been corrected for the resistance of the DCS and are expressed in mA per division.

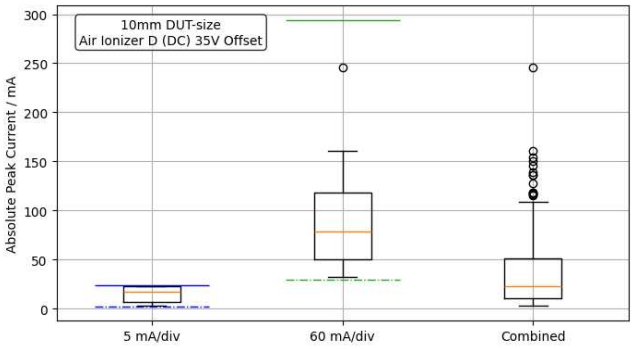

Figure 4: Influence of the oscilloscope's Volts per Division setup on the evaluation of measured peak currents

With a 5 mA/div setting (Fig. 4 on the left), the trigger level is set to 2.5 mA/div (Fig. 4, dash-dot blue line) and all points exceeding 25 mA (Fig. 4, solid blue line) are cut off. With this setup, 75 out of 100 discharges can be triggered. With a broader setup of 60 mA/div (Fig. 4, middle), peak currents of up to 300 mA (Fig. 4, solid green line) can be measured. However, this setting also and yields only 43 triggered pulses out of 100. By combining both measurements (Fig. 4 on the right), it is obvious that the small VpD setup leads the more accurate median value and thus the more accurate representation of the ionizer performance. Therefore, the authors decided to proceed the measurements with low mA/div settings, even though this means not being able to capture the absolute peak currents of some outliers.

III. Measurement results

This section discusses the measurement results. Subsection A introduces the measured transferred charge, transferred energy, and peak currents, and relates the latest to [12]. Subsection B examines the influence of the DUT size, followed by the impact of AC ionizer frequency and DC offset voltage in subsections C and D, respectively. Subsection E highlights the importance of ionizer maintenance. In subsection F., outcomes of measurements with DUTs additionally pre-charged to 100 V are presented. Subsection G. shows measurements with 2 different distances between the DUT and the ionizer. Finally, the origin of the DUT charging is discussed in subsection H.

A. Peak current, transferred charge and transferred energy

Fig. 5 to 7 present the captured absolute peak currents, total amount of charge being transferred and transferred energy, respectively. In all three plots, the smallest DUT size (10 mm) is presented in blue, the medium 15 mm edge length DUT in orange and the largest DUT with the 40 mm edge length in green.

The values for absolute peak currents in Fig. 5 are directly extracted from the captured discharge curves. These are important to estimate the risk for oxide breakdown within the gate of an ESDS device.

The amount of charge being transferred during the discharge (Fig. 6) is the integrated current over time:

$$Q = \int I(t)\, dt \qquad (1)$$

In the context of manufacturing and handling of ESDS devices, the residual charge is a critical performance indicator, as it quantifies the amount of charge remaining on the DUT after ionization. This can reflect both incomplete neutralization of the charge and/or even unintended charging of the DUT caused by the ionizer.

Finally, Fig. 7 depicts the transferred energy during the discharge of the DUT. The transferred energy has been calculated using equation (2):

$$E = R \int I(t)^2 \, dt \qquad (2)$$

The amount of transferred energy may help to estimate the risk for an energy-driven damage, such as metal melting and/or other heat-driven failure mechanisms.

Table 2 summarizes the measured median peak currents and sets them in relation to the pre-charge voltages that produced the same current from [12]. Only the values for 10 mm and 1 mm DUT length can be compared, as 40 mm DUT was not utilized in study [12]. The measured median current values, which are caused by the different ionizers are in the range of 2 V up to 14 V, highlighting the importance of this study, especially for advanced packaging and die to die (D2D) interfaces, for which a CDM target level of 30 V (low-density D2D interfaces), down to 5 V (high-density D2D interfaces) was proposed by the Industry Council on ESD Target Levels in [13].

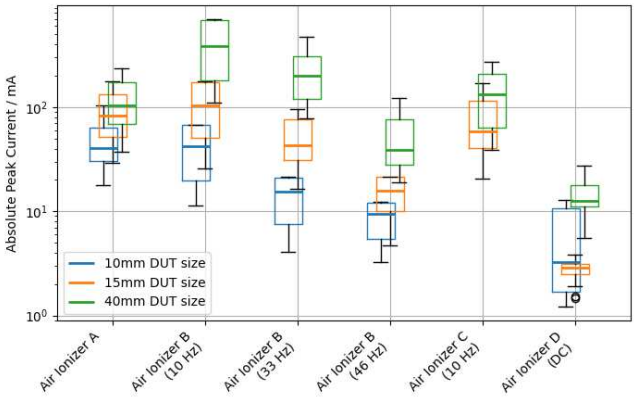

Figure 5: Absolute peak discharge currents measured with the Discharge Current Sensor across different bar ionizers (x-axis) for 10 mm (blue), 15 mm (orange) and 40 mm (green) DUTs

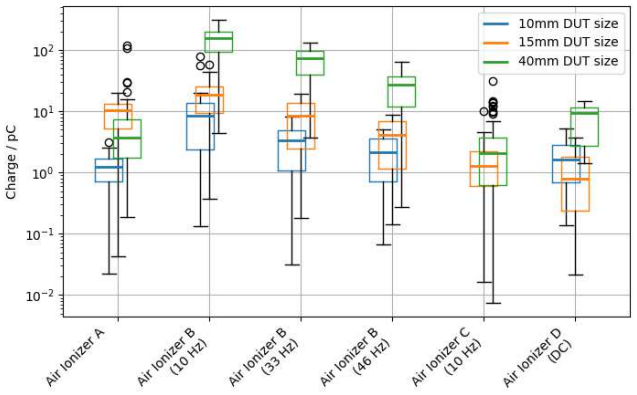

Figure 6: Total amount of charge being transferred during the discharges measured with the Discharge Current Sensor across different bar ionizers (x-axis) for 10 mm (blue), 15 mm (orange) and 40 mm (green) DUTs

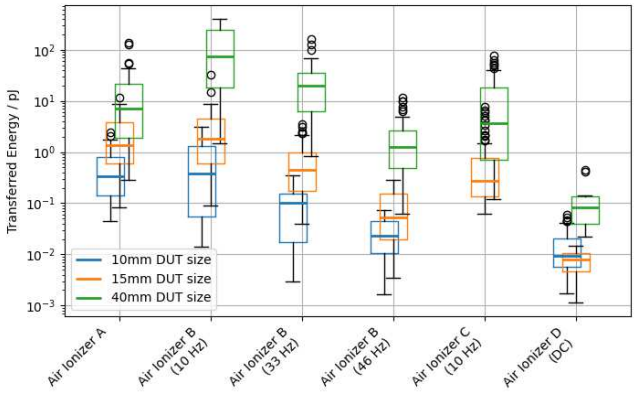

Figure 7: Transferred energy during the discharges measured with the Discharge Current Sensor across different bar ionizers (x-axis) for 10 mm (blue), 15 mm (orange) and 40 mm (green) DUTs

Table 2: Overview of used ionizers

IONIZER	DUT	MEDIAN PEAK CURRENT	CORRESPONDING VOLTAGE FROM [12]
A	10 mm	40.8 mA	5 V to 8 V
A	15 mm	82.6 mA	11 V to 14 V
B 10 HZ	10 mm	42.4 mA	8 V to 11 V
B 10 HZ	15 mm	103 mA	11 V to 14 V
B 33 HZ	10 mm	15.4 mA	2 V to 5 V
B 33 HZ	15 mm	42.9 mA	2 V to 5 V
C 10 HZ	15 mm	58.8 mA	5 V to 11 V
D	10 mm	3.3 mA	2 V to 5 V
D	15 mm	2.9 mA	2 V to 8 V

B. Size of the DUT

From Fig. 5 can be easily derived, that the absolute peak currents increase with increasing DUT size. The only outlier is the measurement with a 10 mm DUT and ionizer D. This measurement (Fig. 5, blue box-and-whisker plot on the far right) was performed with an unmaintained ionizer leading in higher peak currents, charge and energy. This will be discussed more in detail in section E. of this chapter.

The amount of transferred charge, as presented in Fig. 6, also increases with increasing DUT size. A larger DUT not only features larger capacitance

compared to a smaller DUT but also offers more area for the ions to hit its surface. This can lead to higher charge accumulation, especially in a case of disbalanced ionizer. The only exception to this rule is ionizer A (Fig. 6, very left), where the median of the transferred charge of the 15 mm DUT exceeds the median of the transferred charge of the 40 mm DUT. Ionizer A, although being an AC ionizer, uses a different technology than the other AC ionizers B and C. Further investigations into this topic are needed to confirm whether the ionizer type causes this behavior or whether it is a faulty measurement.

Finally, Fig. 7 presents the amount of transferred energy. Again, an increasing DUT size leads to an increased amount of transferred energy, increasing the risk of energy-driven failure in the ESDS device.

C. Influence of the AC ionizer frequency

Fig. 5 to 7 disclose, that the measured absolute peak current, charge and transferred energy increases with decreasing frequency. Moreover, different AC ionizers cause different peak currents and transferred charge and energy.

Therefore, Fig. 8 and 9 compare, on the example of the 15 mm DUT, the absolute peak current values and transferred charge for both AC ionizers with adjustable frequencies used in this study. Ionizer C (Fig. 8 and 9, orange box-and-whisker plots) produced lower median values of peak discharge currents as well as lower transferred charge compared to ionizer B (Fig. 8 and 9, blue box-and-whiskers plots). At 10 Hz, the minimum and maximum measured peak currents are very comparable for both ionizers (Fig. 8, on the left). Interestingly, the transferred charge at the same frequency setting is much lower for ionizer C (Fig. 9 on the left, orange box) than ionizer C (Fig. 9 on the left, blue box). The reason is obvious when looking at the captured discharge current pulses as presented in Fig. 10. When ionizer B (Fig. 10, blue curves) blows towards the 15 mm DUT, the captured discharge current pulses has significantly wider Full Width at Half Maximum (FWHM) compared to the discharge current pulses with ionizer C (Fig. 10, red curves). Wider FWHM at comparable peak current leads to larger area under the curve and thus larger Q. Furthermore, Fig. 10 also reveals that with ionizer B, some of the peak currents were clipped, which would eventually lead in even higher absolute peak currents and transferred charge values for this ionizer at 10 Hz.

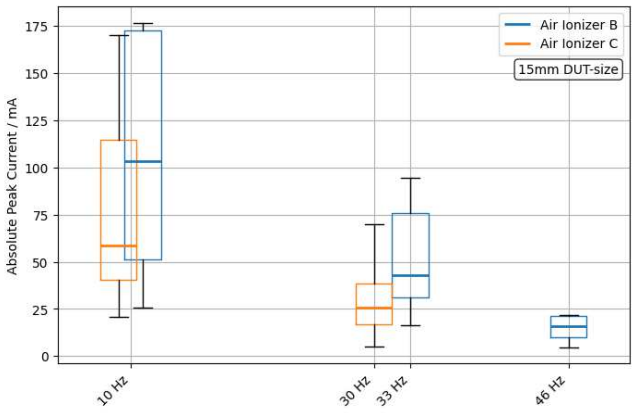

Figure 8: Influence of the AC ionizer frequency on the absolute peak current measured with the Discharge Current Sensor and 15 mm DUT

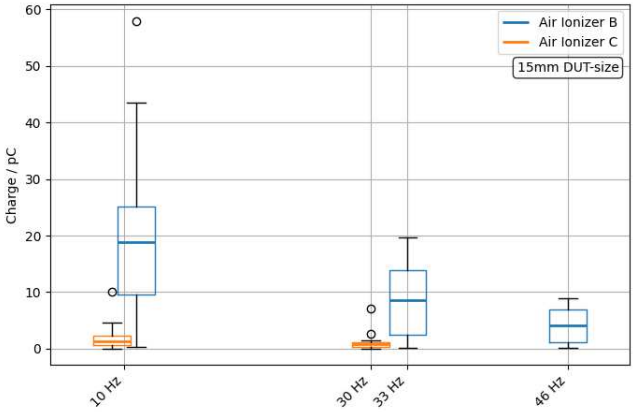

Figure 9: Influence of the AC ionizer frequency on the transferred charge measured with the Discharge Current Sensor and 15 mm DUT

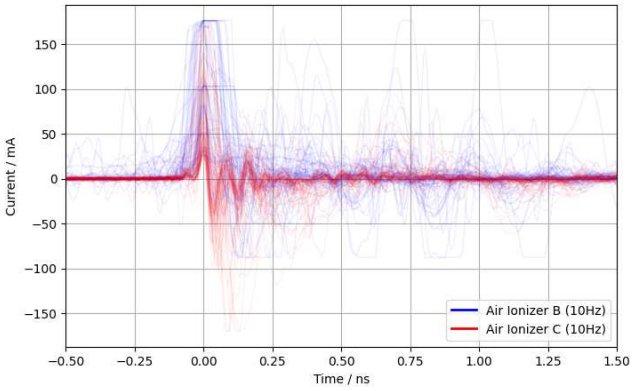

Figure 10: Discharge currents of a 15 mm DUT captured with the Discharge Current Sensor, while ionizer B (blue curves) or ionizer C (red curves) is in operation

D. DC offset

To analyze the influence of the ionizer voltage offset on the discharge current pulses, ionizer D is deployed as it is the only one used in this study allowing to set an offset.

Fig. 11 presents the absolute peak currents for measurement with a 15 mm edge length DUT and a DC ionizer (ionizer D from Table 1). The median peak currents are 2.9 mA with a nominally 0 V offset (Fig. 11, on the left), 18.7 mA in the case 15 V offset (Fig. 11, middle) and finally 30.7 mA when the ionizer is set to 35 V offset (Fig. 11, on the right).

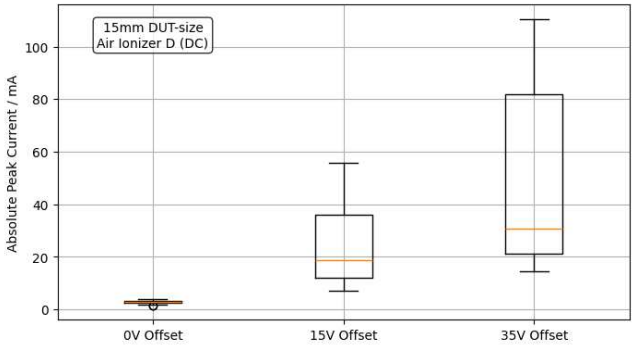

Figure 11: Influence of the DC offset on the absolute peak current measured with the Discharge Current Sensor and 15 mm DUT

The transferred charge depicted in Fig. 12 follows similar trend as the peak current and increases with increasing offset voltage. The median charges from all triggered discharges are 0.8 pC, 5.4 pC and 7 pC for nominally 0 V offset, 15 V offset and 35 V offset respectively.

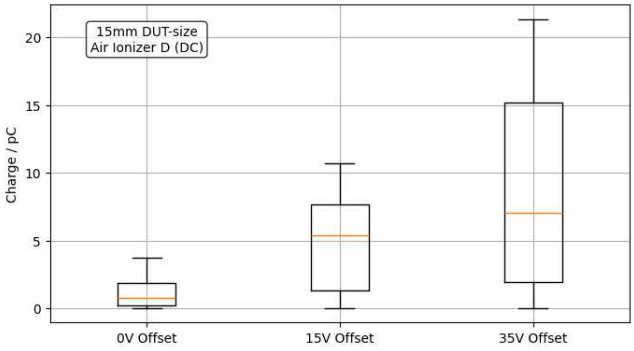

Figure 12: Influence of the DC offset on the transferred charge measured with the Discharge Current Sensor and 15 mm DUT

For the sake of completeness, the energy transferred during the discharges is presented in Fig. 13. The median values are 8 fJ (nominally 0 V offset, Fig. 13 on the left), 93 fJ (15 V offset, Fig. 13 in the middle) and 228 fJ (35 V, Fig.13 on the right).

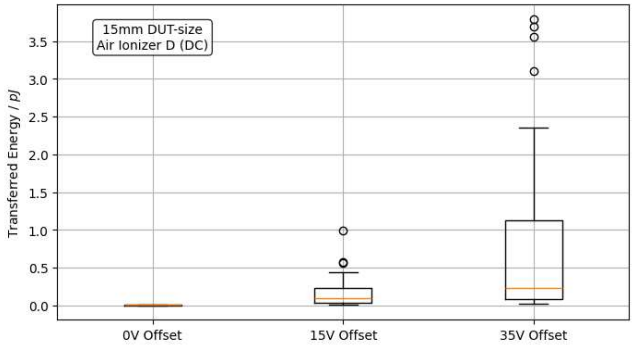

Figure 13: Influence of the DC offset on the transferred energy measured with the Discharge Current Sensor and 15 mm DUT

E. Maintenance of the ionizer

This section highlights the importance of proper and periodical maintenance of an air ionizer. Both measurements are performed with the same DUT size of 15 mm and the same ionizer type (ionizer D from Table 1) placed at the same distance from the DUT. The measurements on the left are conducted with a new ionizer, while the measurement plotted on the right with an old, not maintained ionizer. The peak currents (Fig. 14) as well as the transferred charge (Fig. 15) increases drastically for not-maintained ionizer. As shown in Fig. 14, the median absolute peak current increases by a factor larger than 3 for the unmaintained ionizer (from 2.9 mA to 8.9 mA). The median of transferred charge is more 4.5 times higher for an unmaintained ionizer compared to a new one (3.6 pC and 0.79 pC, respectively). After cleaning the emitter points, the values return almost to the values of a new ionizer.

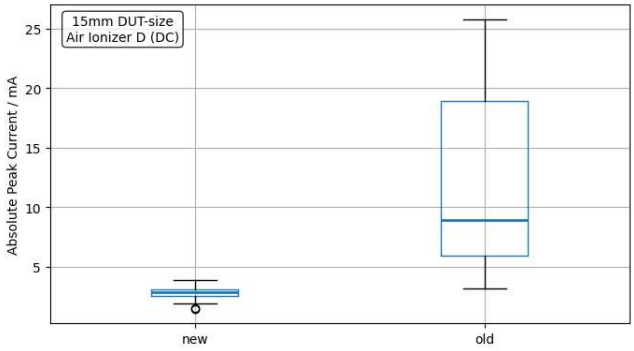

Figure 14: Peak discharge currents for a 15 mm DUT exposed to ionizer D at fixed distance. Left: new ionizer, right: Aged, not-maintained ionizer

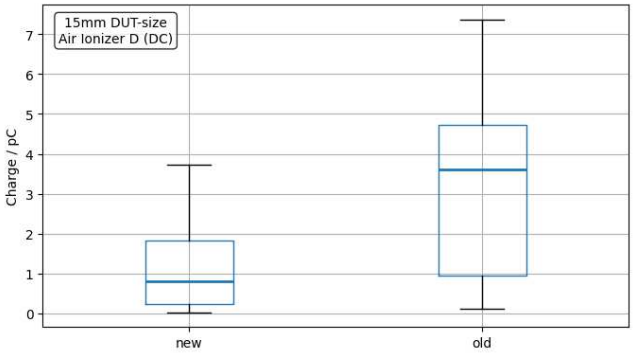

Figure 15: Transferred charge during a discharge of a 15 mm DUT exposed to ionizer D at fixed distance. Left: new ionizer, right: Aged, not-maintained ionizer

F. Pre-charged DUT

In order to evaluate the effectivity of the ionization, the DUT is pre-charged to 100 V using the charging pin of the DCS (Fig. 1 on the right) and subsequently discharged in the discharge pin of the DCS. The ionizer is in operation during the whole process. Fig. 16 presents the measured peak currents with pre-charging of the DUT (orange boxes) compared to the measurements without any pre-charging (blue boxes) for all ionizers from Table 1 and 15 mm DUT. Fig. 17 and Fig. 18 follow the same color-coding and depict the transferred charge in pC (Fig. 17) and the transferred energy in pJ (Fig. 18).

From the plots, it is obvious that the median peak current (Fig. 16) and the median of total amount of transferred charge (Fig. 17) slightly decrease in the case of additionally pre-charging the DUT. There are two possible reasons for this phenomenon. Firstly, the pre-charging of the DUT deposits charge carriers on the DUT generating an electric field. This electric field actively attracts ions of opposite polarity emitted by the ionizer toward the charged surface, which enhances ion transport efficiency and leads to more efficient charge neutralization compared to field-free (not pre-charged) conditions. Secondly, due to the additional step of charging, there is more time for the ionizer to better neutralize the charge. Specifically, the interval between two subsequent discharges increases from approximately 0.5 s to 2 s. To decouple these two effects, additional measurements should be conducted in the future using the same movement and timing pattern but with the charging pin floating, in order to determine whether the extended exposure time or the improved ion attraction or combination of both is the dominant factor.

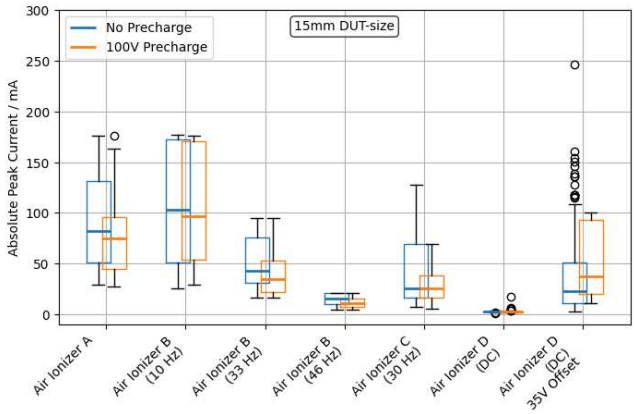

Figure 16: Absolute peak discharge currents measured with the Discharge Current Sensor across different bar ionizers (x-axis) for a 15 mm DUT, without pre-charging (blue boxes) and with pre-charging the DUT to 100 V (orange boxes)

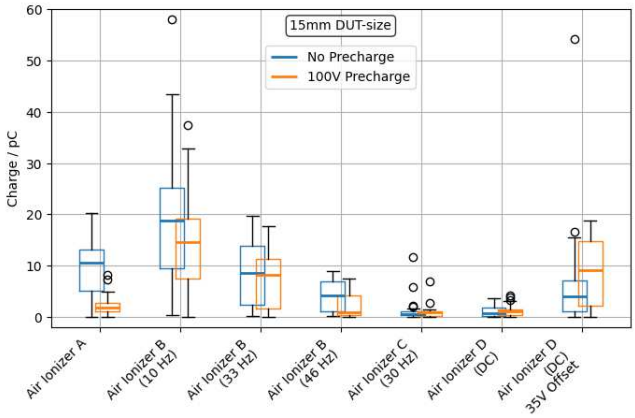

Figure 17: Total amount of charge being transferred during the discharges measured with the Discharge Current Sensor across different bar ionizers (x-axis) for a 15 mm DUT, without pre-charging (blue boxes) and with pre-charging the DUT to 100 V (orange boxes)

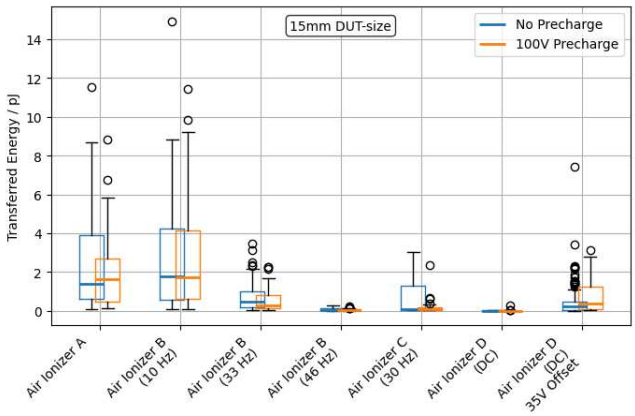

Figure 18: Transferred energy during the discharges measured with the Discharge Current Sensor across different bar ionizers (x-axis) for a 15 mm DUT, without pre-charging (blue boxes) and with pre-charging the DUT to 100 V (orange boxes)

G. Influence of the distance between ionizer and DUT

Fig. 19 and 20 illustrate the influence of ionizer-to-DUT distance on peak discharge currents and transferred charge, respectively. The distance between the DUT and ionizer C was increased from 15 cm to 20 cm. While the minimum and maximum values remain largely unchanged, the median peak current increases with increasing distance (Fig. 19). A similar trend is observed for the amount of transferred charge in the case of ionizer C operating at 10 Hz (Fig. 20, blue). However, at the higher frequency setting of 30 Hz, the median transferred charge decreases from 0.9 pC to 0.5 pC with increasing distance (Fig. 20, orange). These results suggest that, for some configurations, greater distances may lead to higher electrical stress on ESDS during ionization. Further research is required to establish a safe operating zone that ensures efficient charge neutralization while maintaining peak currents and transferred charge as low as possible.

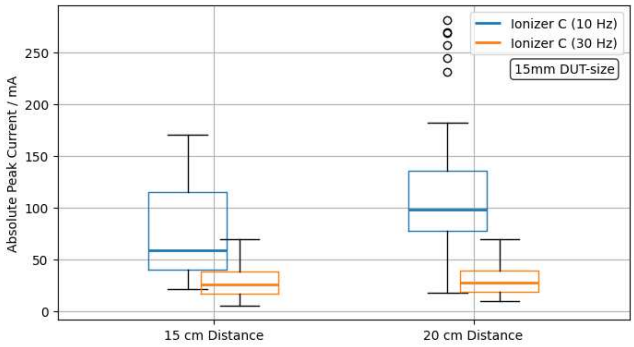

Figure 19: Influence of the distance between the DUT and the ionizer on the peak current caused by ionizer C

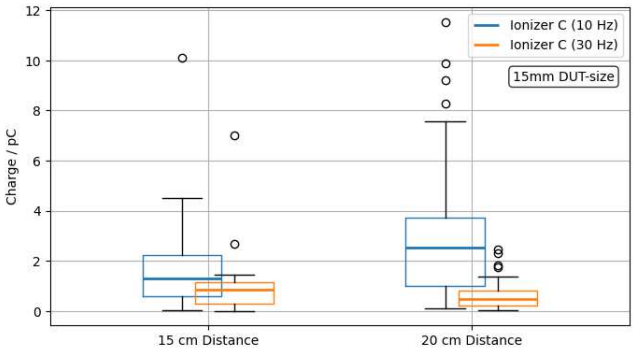

Figure 20: Influence of the distance between the DUT and the ionizer on the transferred charge caused by ionizer C

Notably, the distance dependence of the peak current and transferred charge also raises a more fundamental question: whether the observed charging of the DUT is caused by actual ion deposition or by electrostatic induction from the alternating electric field of the AC ionizer. The answer to this question is of significant importance for ESD risk assessment, particularly for die-to-die interfaces [13].

H. Ion transfer vs induction from fast changing AC fields

For this reason, an additional measurement setup utilizing a single-nozzle AC ionizer (not listed in Table 1) is designed to distinguish between conductive charge transfer through ion deposition and induction caused by the electric field of the AC ionizer. The nozzle of the AC ionizer is facing the DUT directly at a distance of 15 cm. The largest DUT with an edge length of 40 mm is used, as it exhibited the highest peak currents and transferred charge in the prior measurements. Three types of measurements are performed to pinpoint the origin of the charging: (1) with the ionizer and air pressure on, (2) with the ionizer on but the air pressure turned off, and (3) with the ionizer on and air pressure off, while the ionizing nozzle is additionally blocked with an FR4 sheet. Furthermore, a reference measurement is performed with the ionizer completely turned off to ensure no additional charging source is present nearby. The outcomes of these measurements are summarized in Fig. 21 (peak current) and Fig. 22 (transferred charge).

Under normal operating conditions (ionizer and air pressure on), the highest peak currents and transferred charge are observed (Figs. 21 and 22 on the left). When the air pressure is switched off while the ionizer remains active, ions are no longer actively transported away from the needle tip towards the DUT. If DUT charging was primarily caused by conductive transfer through ion deposition, a significant reduction in peak current and transferred charge would be expected. However, the observed decrease is not so distinctive, which can possibly be attributed to ion-ion repulsion still driving a residual ion flow toward the DUT even in the absence of pressurized air (Fig. 21 and 22, second from the left).

Consequently, this measurement alone does not allow a definitive conclusion regarding the dominant charging mechanism. To further isolate the effect, an FR4 sheet is placed in front of the nozzle, physically blocking ion transport while allowing the alternating electric field to reach the DUT, as FR4 is not electrically conductive. Under this condition, both peak current and transferred charge drop significantly (Fig. 21 and 22, right). This strongly suggests that the charging of the DUT is primarily caused by ion deposition rather than by electrostatic induction from the electric field of the AC ionizer.

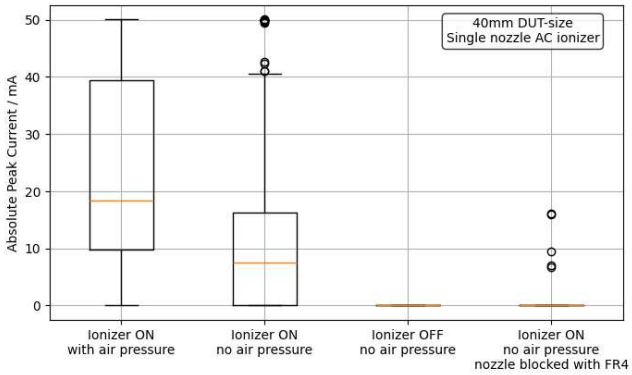

Figure 21: Peak discharge currents measured under different ionizer operating condition for the 40 mm DUT at 15 cm distance

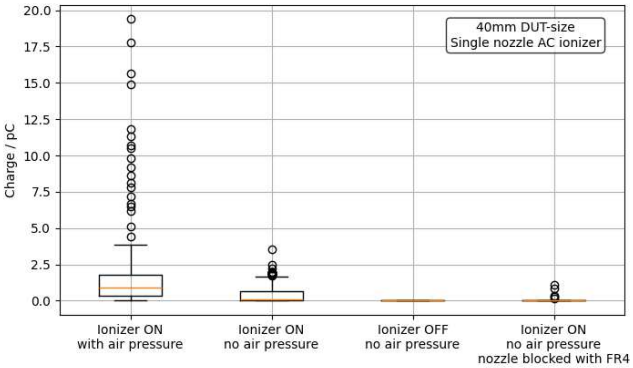

Figure 22: Transferred charge measured under different ionizer operating condition for the 40 mm DUT at 15 cm distance

IV. Conclusion

This paper shows an alternative approach to use the discharge current sensor introduced in [11] and [12]. Peak currents, transferred charge, and transferred energy caused by various AC and a DC ionizer on 3 different DUT sizes are reported. It is shown that these values increase with increasing DUT size. Furthermore, the influence of AC ionizer frequency is investigated, revealing lower values at higher AC frequencies. The importance of a carefully adjusted DC offset as well as proper and periodical maintenance of ionizers has been highlighted. The measurements demonstrated an improved ionization efficiency for purposely pre-charged DUTs. Finally, the origin of charging (ion flux or AC fields) was investigated, suggesting that the charging of the DUTs caused by an ionizer is primary due to the ion deposition.

The presented measurements show that this method can be utilized as additional check for ionizer balancing by measuring the discharge currents caused by charge accumulated on the aluminum plate (DUT). Moreover, the presence of other possible charging sources, such as electric field coupling from the ionizer, can be detected. To control the efficiency of an ionizer, measurements can be carried out with pre-charging the DUT and subsequently discharging it while the ionizer is operating. This approach can serve as a valuable addition to the standardized measurements with a charged plate monitor as described in [1-4], especially when the performance of the ionizer on small DUTs over short time spans and at very low offset voltages is of interest.

As an outlook, measurements with different ionizer types (e.g. nozzle, fan) as well as from various manufacturers could be performed to assess their applicability for modern manufacturing processes. Furthermore, the position of the ionizer with respect to the DUT should be investigated to determine the safest operating distance.

V. Acknowledgements

The authors want to express their gratitude to Jay Skolnik for his great mentoring and valuable contributions to this paper and the Cisco University Research Program Fund, a corporate advised fund of Silicon Valley Community Foundation, for partially funding this work with the Grant 368789 - Award Letter - GB-1636436 - 2025-12-05 11-03.

Furthermore, parts of the work presented were carried out in the framework of the APECS Pilot Line of the Chips Joint Undertaking, funded by Horizon Europe (ID: 101183307) and digital Europe (ID: 101182906) Programs and national funding authorities of Austria, Belgium, Finland, France, Germany, Greece, Portugal, Spain.

VI. References

[1] ANSI/ESD S20.20-2021 ESD Association Standard for the Development of an Electrostatic Discharge Control Program for Protection of Electrical and Electronic Parts, Assemblies, and Equipment (Excluding Electrically Initiated Explosive Devices).

[2] ESD TR20.20-2016 ESD Association Technical Report for the Protection of Electrostatic Discharge Susceptible Items, Handbook for the Development of an Electrostatic Discharge Control Program for the Protection of Electrical Parts, Assemblies, and Equipment.

[3] ANSI/ESD STM3.1-2015 ESD Association Standard Test Method for the Protection of Electrostatic Discharge Susceptible Items, Ionization.

[4] ANSI/ESD SP3.3-2016 ESD Association Standard Practice for the Protection of Electrostatic Discharge Susceptible Items-, Periodic Verification of Air Ionizers.

[5] ANSI/ESD SP3.4-2016 ESD Association Standard Practice for the Protection of Electrostatic Discharge

Susceptible Items-, Periodic Verification of Air Ionizer Performance Using a Small Test Fixture.

[6] V. Kraz, “Notes on Maintaining Sub-1V Balance of an Ionizer,” in 2004 26th Annual EOS/ESD Symposium (EOS/ESD), 2004.

[7] J. Yoo and E. Koo, “ESD Risk Analysis using Pulsed AC Ionization Technology,” presentation at 2018 EOS/ESD Manufacturing Symposium, 2018.

[8] J. Yoo, E. Choi and E. Koo, “CPM Test Limitation Study for AC, Pulsed AC and High Frequency AC Ionizers vs. DC Based Ionizers,” in 2019 41th Annual EOS/ESD Symposium (EOS/ESD), 2019.

[9] J. Yoo and A. Steinman, “Alternative Measurement Methodology for Fast switching AC Ionizer Offset Voltage Measurement,” in 2023 45th Annual EOS/ESD Symposium (EOS/ESD), 2023.

[10] S. Cooray, T. Sato, K. Okano, and T. Terashige, “Basic Characteristics of the Field Assisted Air Ionizer,” in 2013 35th Annual EOS/ESD Symposium (EOS/ESD), 2013.

[11] E. Jirutková, H. Wolf and H. Gieser, “In-situ ESD current sensing in a pick and place machine,” in 2024 46th Annual EOS/ESD Symposium (EOS/ESD), 2024.

[12] E. Merkel, H. Wolf and L. Heiland, “Discharge Currents of Metallized Silicon Chiplets at Low Pre-Charge Voltages,” in 2025 47th Annual EOS/ESD Symposium (EOS/ESD), 2025.

[13] Industry Council on ESD Target Levels, “White Paper 2: A Case for Lowering Component Level CDM ESD Specifications and Requirements Part II: Die-to-Die Interfaces”: https://www.esdindustrycouncil.org/ic/en/documents